JOURNAL OF MATERIALS SCIENCE **38** (2003) 2935–2944

Hot shock compaction of nanocrystalline alumina

G. J. VENZ, P. D. KILLEN
Centre for Medical, Health and Environmental Physics, Queensland University of Technology, Brisbane, QLD 4001, Australia
E-mail: garyvenz@hotmail.com

N. W. PAGE
Department of Mechanical Engineering, University of Newcastle, Newcastle, NSW 2308, Australia

An experimental investigation of hot shock compaction of a nanocrystalline alumina powder was performed. The effects of variations in shock pressure and compaction temperature on the properties of the compacted materials were studied. It was found that the bulk density and hardness of the compacted material increased with shock pressure. Increasing compaction temperature resulted in increases in compact hardness and bonding, and reductions in cracking within the compacted specimens. The results suggest that dense, well bonded, crack free nanocrystalline ceramics may be fabricated more effectively using hot shock compaction, than by room temperature shock compaction followed by sintering or room temperature static compaction followed by sintering.

1. Introduction

The properties of nanocrystalline ceramics have been shown to be superior to those of conventional microcrystalline ceramics in a number of ways. These include increased ductility and plastic deformation, improved sintering behaviour, and increased strength and hardness [1–4]. It is difficult to produce bulk nanocrystalline ceramic materials using traditional powder processing techniques such as sintering, as these techniques often require the material to be exposed to elevated temperatures for extended periods of time. This leads to crystal growth within the material, thus destroying the desired nanocrystalline microstructure. One method which has been proposed for the production of nanocrystalline ceramics is shock compaction.

Shock compaction is essentially a rigid die pressing technique in which consolidation is achieved by the propagation of a shock wave through the material. The shock wave may be initiated either by the detonation of an explosive charge in contact with or near the target material, or the impact of a high-speed projectile or flyer plate onto the target material. The projectile or flyer plate may be accelerated to the desired impact velocity by either the rapid expansion of a compressed gas, or detonation of an explosive.

In the case of powdered materials, propagation of the shock wave through the material results in collapsing of the voids between particles, thus increasing the density of the material. As the powder is compressed, friction between the powder particles results in localized heating at the particle surfaces. After passage of the shock wave, heat is conducted from the surface to the interior of the particles resulting in an increase in temperature of the bulk material. The material then eventually returns to ambient temperature and pressure conditions.

High energy deposition in the powders during compaction leads to the possibility of obtaining very high densities (i.e., $>90\%$) [5, 6]. This is highly desirable if post-compaction sintering is to be performed, as linear shrinkage (and therefore warping and cracking) decrease with increasing green density, enabling increased accuracy in dimensional tolerances. Additionally, the sintering rate increases with increasing green density, reducing the sintering times and/or temperatures required [7]. The high energy deposition also allows for the compaction of powders which are normally very difficult to consolidate by conventional methods [6, 8]. The high rates of heating and subsequent cooling (10^8–10^{11} $K \cdot s^{-1}$ for metals) [9] which occur during the compaction process (i.e., densification, particle surface melting, resolidification, surface cooling) mean that grain growth may be minimised, whilst desirable metastable properties may be retained during and after compaction [5].

When consolidating metal powders, the temperatures and pressures established at the particle surfaces are usually sufficient to induce surface deformation or melting, which assist in densification and bonding of the powder particles. Ceramic materials, however, usually have much higher hardness and melting points than metals. The pressure and temperature conditions produced during compaction are not normally high enough to induce surface deformation and/or melting, and hence sufficient densification and interparticle bonding do not occur. (Meyers *et al*. [10] predicted the pressure required for room temperature shock consolidation of Al_2O_3 powder to be approximately 23 GPa.)

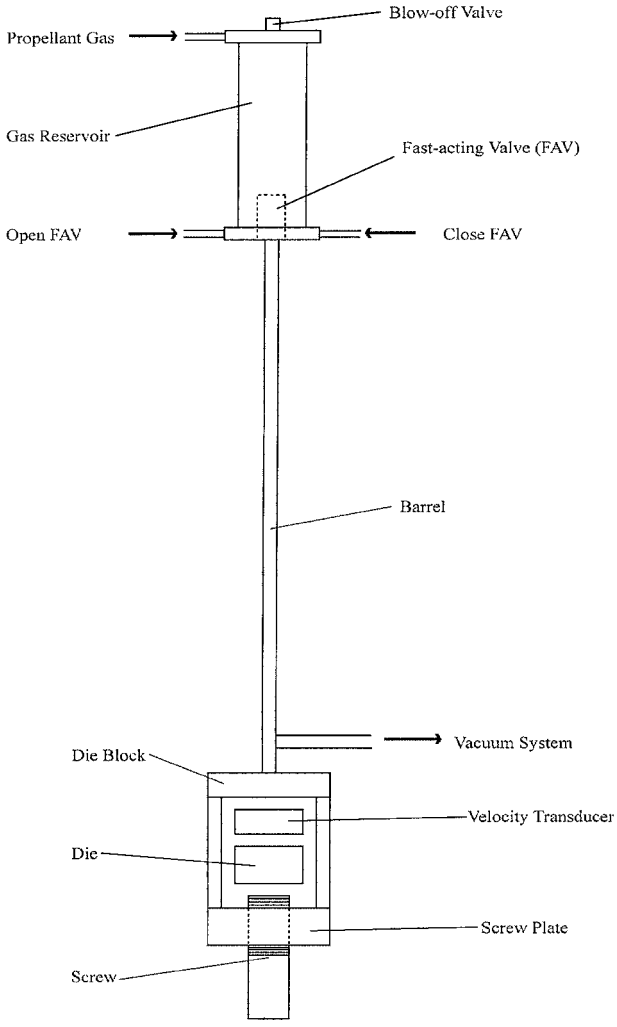

Figure 1 Single stage light gas gun.

It may therefore be necessary to pre-heat the material before compaction. By increasing the thermal energy initially contained in the material, the additional energy deposited in the material by the shock wave should be sufficient to produce adequate densification and bonding. The process of dynamically compacting a pre-heated sample is known as hot shock compaction.

By compacting pre-heated materials, the temperatures achieved at the particle surfaces will be greater than those achieved during ordinary shock compaction. Therefore, it is expected that the temperature-pressure conditions may be sufficient to allow plastic deformation and/or surface melting to occur in ceramic materials, leading to increased densification and interparticle bonding. Furthermore, pre-heating the material results in a reduction of both the powder strength, and the shock energy required to consolidate the powder [11]. This is advantageous, because if excessively large shock energies are used, cracking (a significant and common problem in the shock compaction of ceramics), and material damage are likely to occur. Therefore, by using the appropriate combination of pre-compaction temperature and shock energy, hot shock compaction should be an effective method by which dense, well bonded, crack free materials may be produced [12].

A number of studies have been carried out on the shock consolidation of microcrystalline powdered materials at elevated temperatures [13–15]. The purpose of the current study was to determine the effect of variations in shock pressure and compaction temperature on the properties of materials produced by hot shock compaction of nanocrystalline alumina powder. The properties of interest included final density, bonding, and the presence of cracking.

2. Experimental procedure

2.1. Powder characterization

The powder used in this study was NanoTek® alumina (Al_2O_3), produced by Nanophase Technologies Corporation USA. The grain growth behaviour of the powder at elevated temperatures was studied. Samples of the powder were heated in air for 2 h at 600, 800, 1000 and 1200°C, and for 24 h at 1100°C, removed from the furnace and allowed to cool. Transmission electron

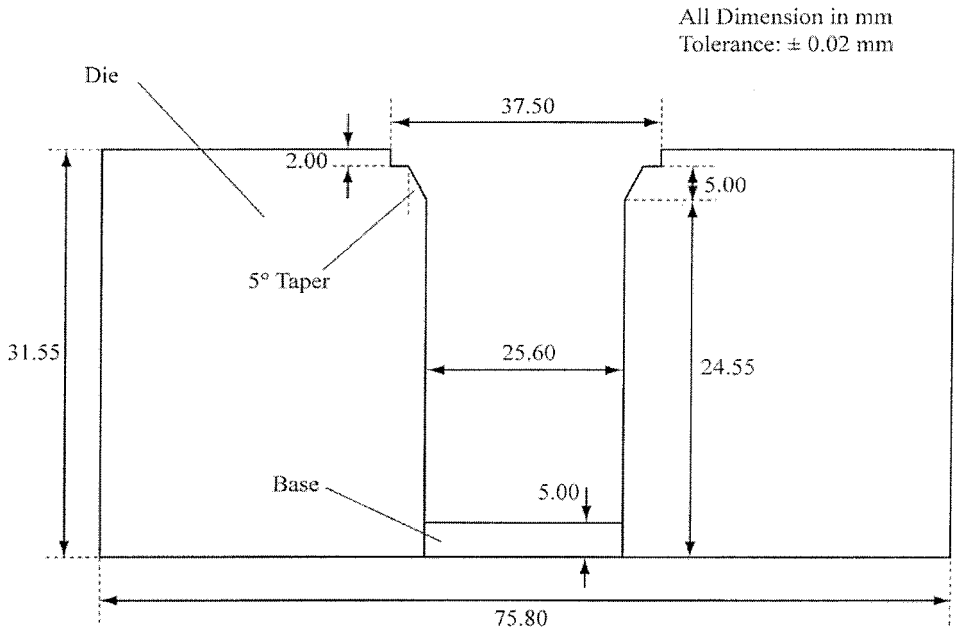

Figure 2 Disposable stainless steel die.

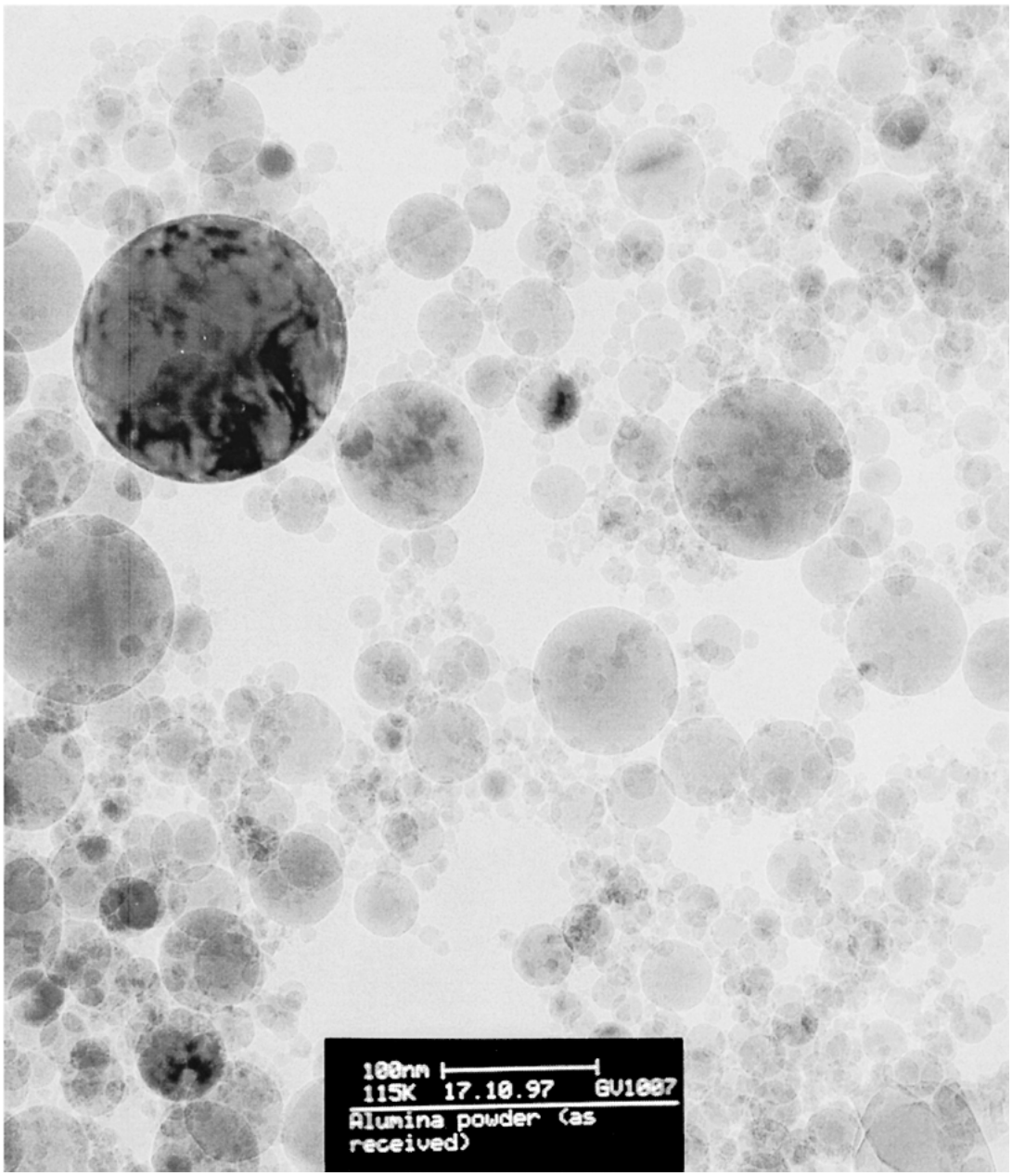

Figure 3 Transmission electron micrograph of NanoTek® alumina powder as received, mag ×115000.

micrographs were taken of the as received powder, and of each heat-treated sample to determine the temperature at which significant grain growth began to occur. This allowed the maximum pre-compaction temperature to be determined.

The quasi-static loading behaviour of the powder in the low-pressure regime was studied. This was achieved by obtaining pressure-density data for quasi-static, uniaxial compaction of the powder in a 25.5 mm diameter cylindrical die. The Chen-Malghan equation [16] shown below was then fitted to the experimental data, and the model parameters obtained from this quasi-static loading behaviour were later used in the calculation of shock pressures and temperatures.

$$V = a_1 + (V_\infty - a_1)\exp\left(\frac{1}{1 + a_3 P}\right) + \left(\frac{(V_0 - a_1) + e(a_1 - V_\infty)}{1 + a_5 P}\right)$$

where, $V =$ specific volume at pressure, $V_0 =$ specific volume at zero pressure, $V_\infty =$ specific volume at large apparent pressure, $P =$ pressure, and $a_i =$ model parameters (where $i = 1$ to 5).

2.2. Hot shock compaction

Hot shock compaction experiments were performed by preheating the powder to temperatures of 500, 600, 700, 800 and 1000°C before compaction. Shock wave generation was achieved using aluminium projectiles (length 50 mm, ∅ 25 mm) launched using a single stage light gas gun at QUT, as shown in Fig. 1 (the gas gun and its operation have been described previously [17], although some modifications have been made to accommodate higher driver gas pressures (up to 15 Mpa) and a longer barrel (3.0 m) which provide projectile velocities up to 720 m/s). Projectile velocities achieved in this study ranged from 330 to 420 m/s. The initial powder density was kept constant at 212 kg/m^3, or 5.9% solid

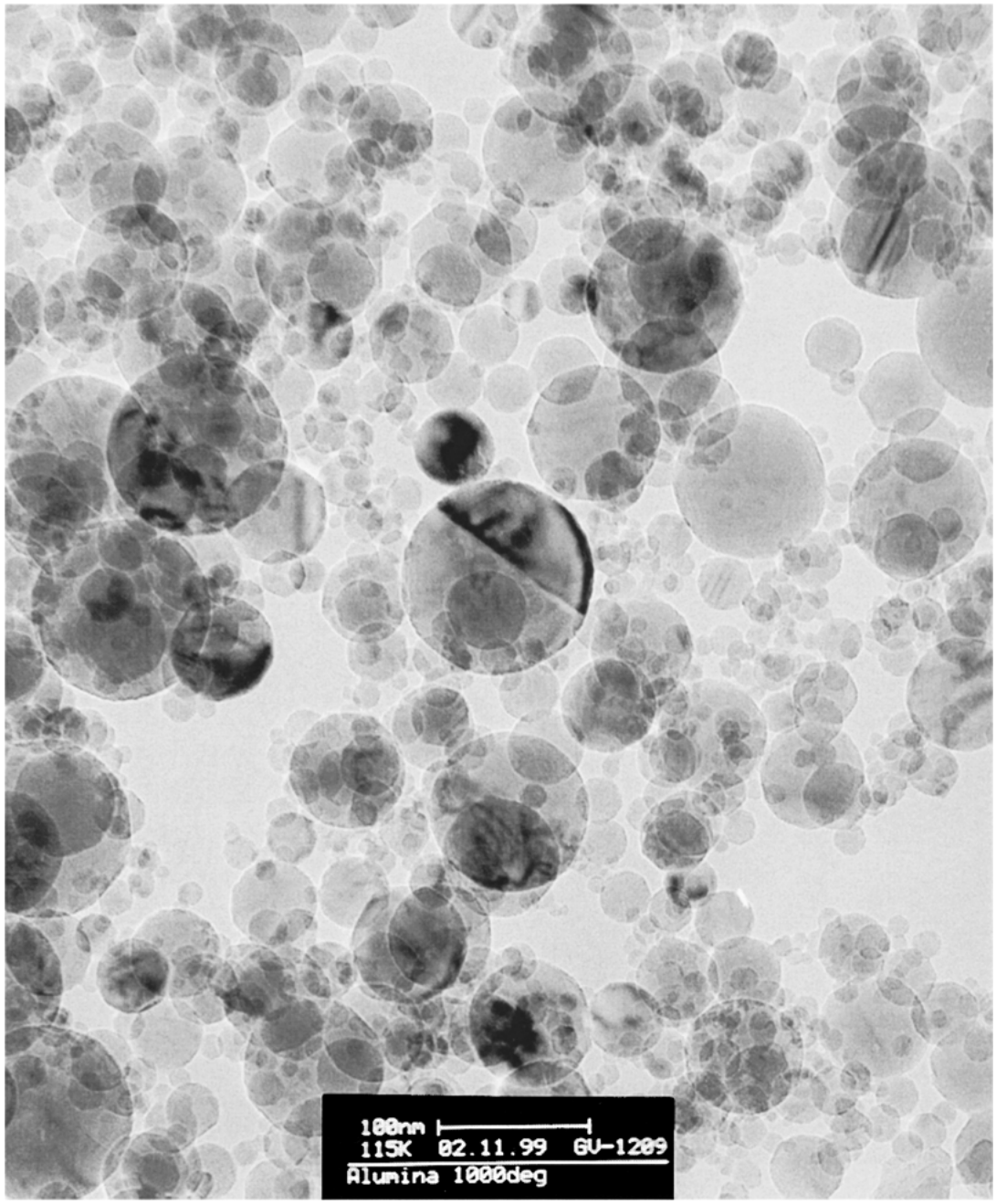

Figure 4 Transmission electron micrograph of powder heated to 1000°C for 2 h, mag ×115000.

density, for all experiments. This resulted in calculated primary shock pressures of 46 to 74 MPa in the powder.

The sample powder was contained in a disposable stainless steel die as shown in Fig. 2. The hot shock compaction experiments were performed by first placing the die containing the powder in a furnace.

Upon reaching the desired temperature, the die was removed from the furnace, placed in the gas gun, and the projectile launched. A number of room temperature shock compaction experiments were also performed.

A number of calibration measurements were performed, showing the variation in powder temperature with time since removing the die from the furnace. This was done for each of the furnace temperatures used. The temperature of the powder at the time of projectile impact was then calculated for each shot using the given furnace temperature, and the time elapsed between removing the die from the furnace and projectile impact.

The compacted materials obtained from these experiments were removed from the dies and broken into several fragments. Density measurements were performed on fragments from each sample using a specific density bottle, with paraffin oil as the immersion fluid.

Microhardness values were obtained for each compact using a UMIS (Ultra Micro-Indentation System) 2000 nanoindenter. Sample fragments were mounted in Lucite, and the sample surface polished using 3–7 μm diamond polish to produce a flat, scratch-free surface. Hardness tests were performed at approximately 25 locations on the surface of each sample. The hardness at each location was calculated from force-penetration data (obtained using a Berkovich indenter), and the mean hardness of each sample calculated.

A number of fragments from the compacts produced by room temperature static and shock compaction were sintered in air for approximately 30 min at temperatures

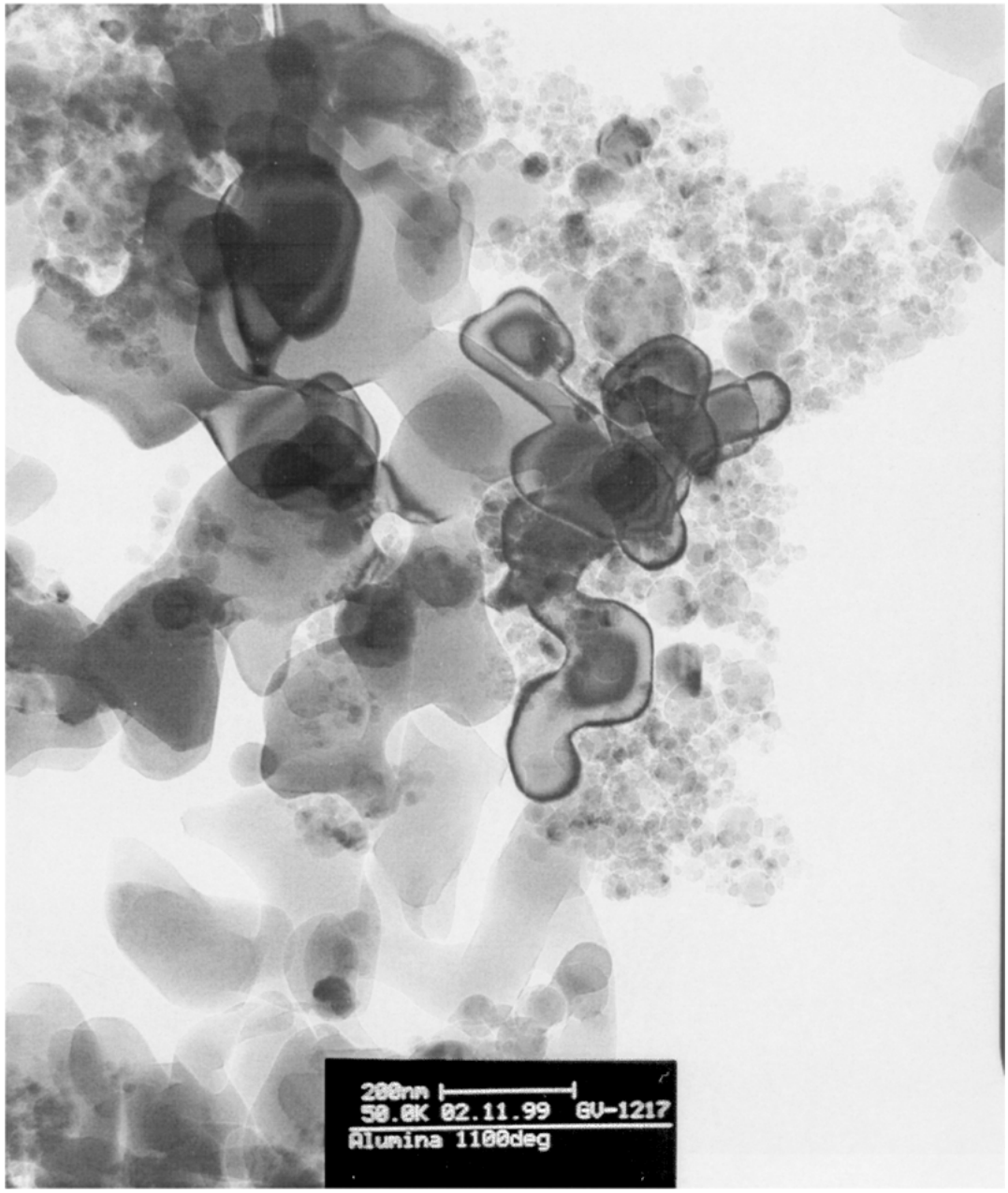

Figure 5 Transmission electron micrograph of powder heated to 1100°C for 24 h, mag ×50000.

of 300, 500, 600, 700, 800, and 1000°C. Microhardness tests were also performed on these sintered samples.

3. Results

Fig. 3 shows a transmission electron micrograph of the as-received powder. It can be seen from this figure that the powder had a spherical morphology, with particle size ranging from approximately 5 to 180 nm. Micrographs of the powders heated to 600 and 800°C for 2 h exhibited no observable grain growth. Comparison of Figs 3 and 4 shows that heating to 1000°C for 2 h resulted in slight changes in the previously spherical particle shape, and small amounts of particle fusion. Fig. 5 shows that heating to 1100°C for 24 h resulted in significant grain growth and fusion of powder particles. Fig. 6 shows further progression of this growth and fusion at 1200°C. These results suggested that the powder should not be preheated to temperatures greater than 1000°C if the nanocrystalline grain structure was to be retained.

Fig. 7 shows the experimental quasi-static loading curves obtained for the powder, and the fits obtained using the Chen-Malghan equation (dashed lines). As Fig. 7 shows, the fit obtained was unacceptable when the initial specific volume (V_0) and solid phase specific volume (V_∞) were fixed at the known values. By allowing V_∞ to vary as a model parameter in the equation, much better agreement with experimental data was obtained. Using the parameters obtained from this equation, together with the initial density of the powder and the projectile parameters (i.e., acoustic impedance and impact velocity), the primary shock pressure and shock induced temperature increase were calculated for each compaction experiment using the 'Wave53c' program [18–20]. The compaction temperature was then calculated from the temperature of the powder before compaction, and the increase in temperature due to

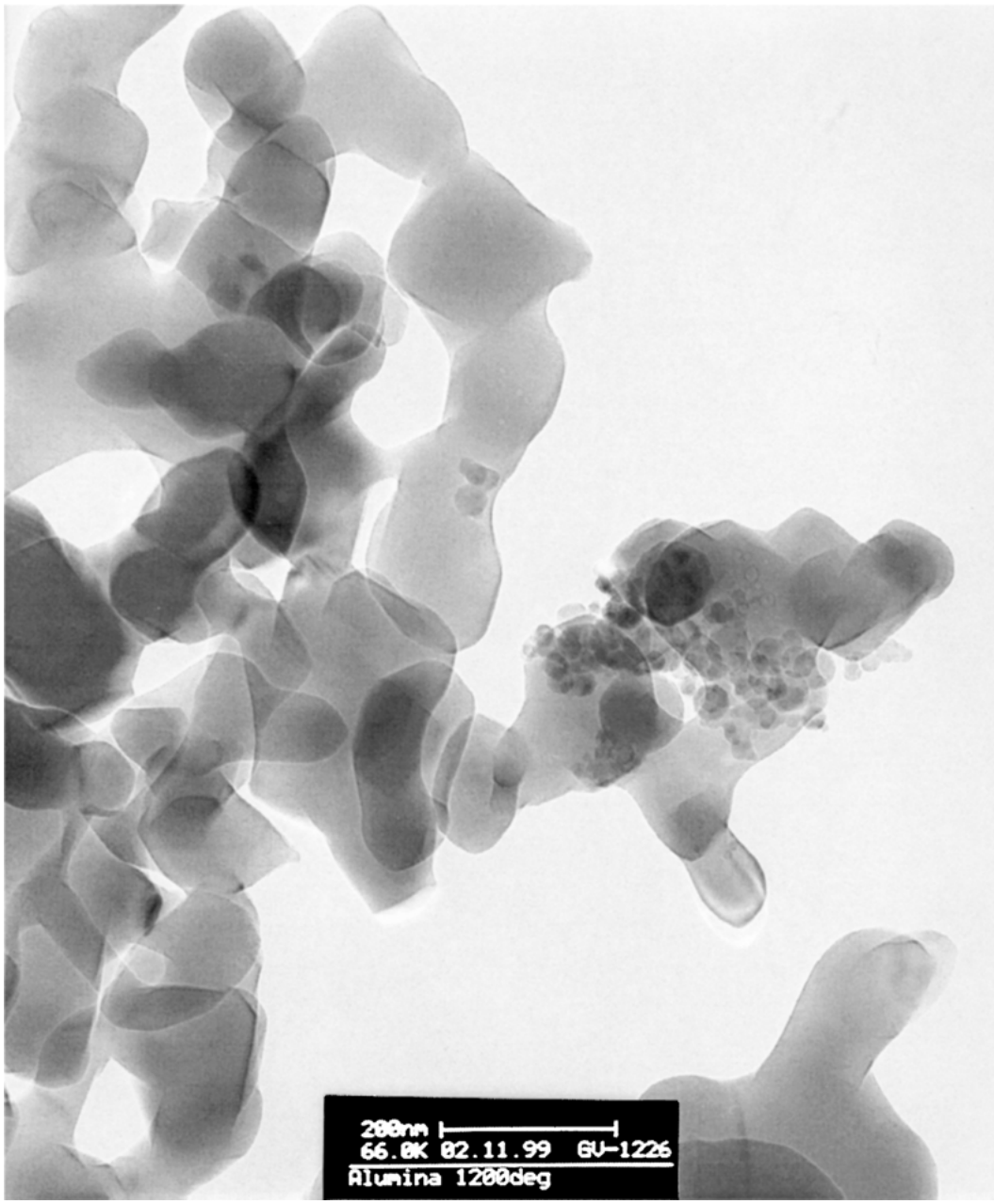

Figure 6 Transmission electron micrograph of powder heated to 1200°C for 2 h, mag ×66000.

the passage of the primary shock wave through the powder.

Figs 8 and 9 are photographs of the sample surface for compacts produced at 467 ± 9°C and 733 ± 20°C respectively. These figures clearly show a reduction in cracking within the compact as compaction temperature increased.

The density results obtained for each compact are presented in Fig. 10 as a function of shock pressure. Due to the small fragments available for testing, the density results contained a large degree of uncertainty. Analysis revealed that there is a statistically significant increase in final bulk density with primary shock pressure. This seems reasonable, as increased shock pressures would result in increased energy deposition within the powder. This, in turn, would lead to greater particle rearrangement and increased final densities. However, there was no significant relationship between density and compaction temperature. This indicated that the temperature conditions achieved in this study were not sufficient to produce plastic deformation of the powder particles during compaction.

The hardness values obtained for the shock compacted samples are shown in Fig. 11 as a function of compaction temperature. It can be seen that there is a positive correlation between compact hardness and

TABLE I Regression results for compact hardness

	Regression	
Parameter	Hardness vs. temperature	Hardness vs. (temperature & pressure)
R	0.72	0.80
R^2	0.52	0.64
p-value	1.58×10^{-6}	1.26×10^{-7}
Standard error	0.39	0.35
Observations	34	34

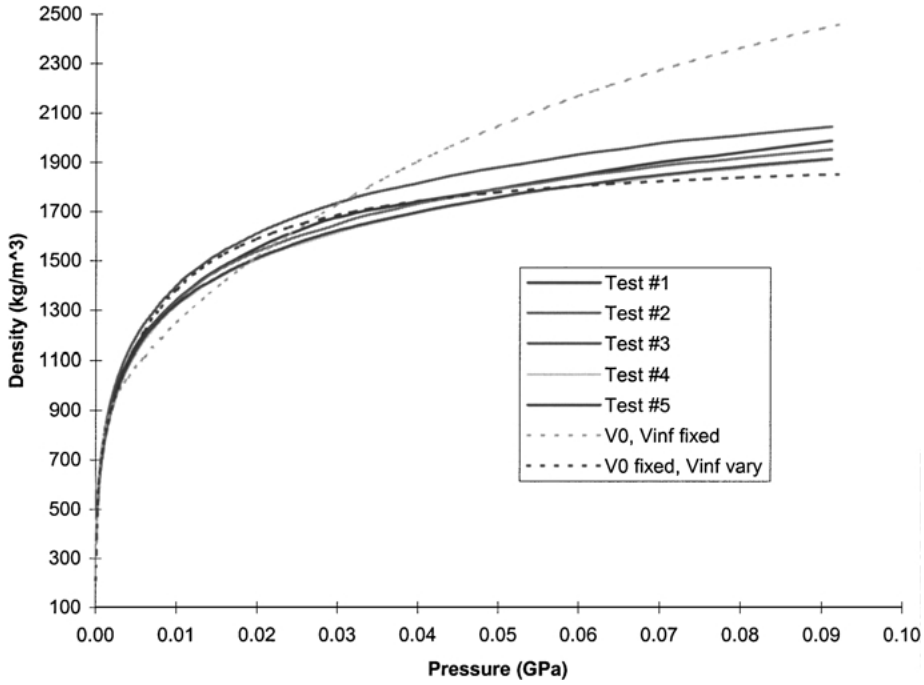

Figure 7 Quasi-static loading curve for alumina powder.

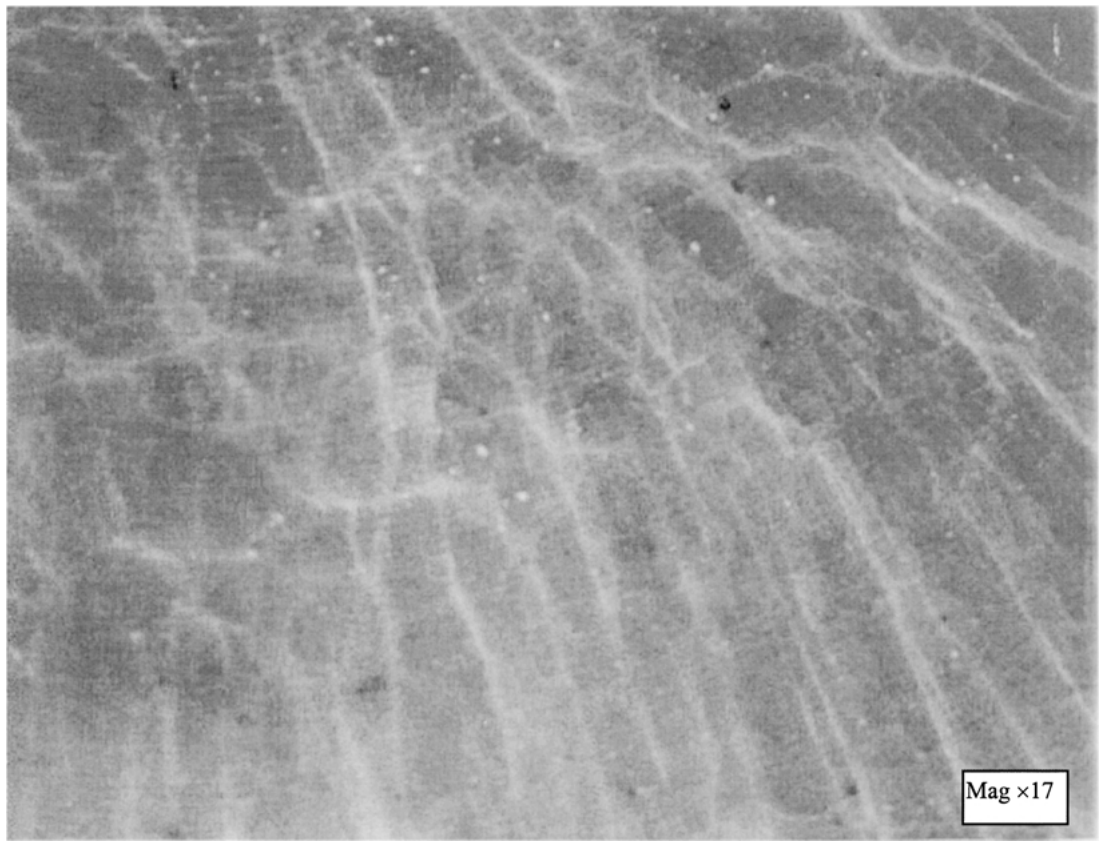

Figure 8 Optical micrograph of sample surface, compaction temperature $467 \pm 9^{\circ}$C.

temperature. Furthermore, adding shock pressure to a multiple regression model significantly improved the model. The results of this multiple regression are given in Table I. These results showed that compact hardness was dependent upon both compaction temperature and shock pressure, with compaction temperature being the more significant of the two. This indicated that, as compaction temperature and shock pressure increased, greater bonding was achieved between powder particles in the compact. The most likely reason for this observation was that the elevated temperatures resulted in increased diffusion across boundaries between neighbouring powder particles, resulting in greater bonding (i.e., increased sintering).

Fig. 12 shows the hardness results for the hot shock compacted samples, together with those for the

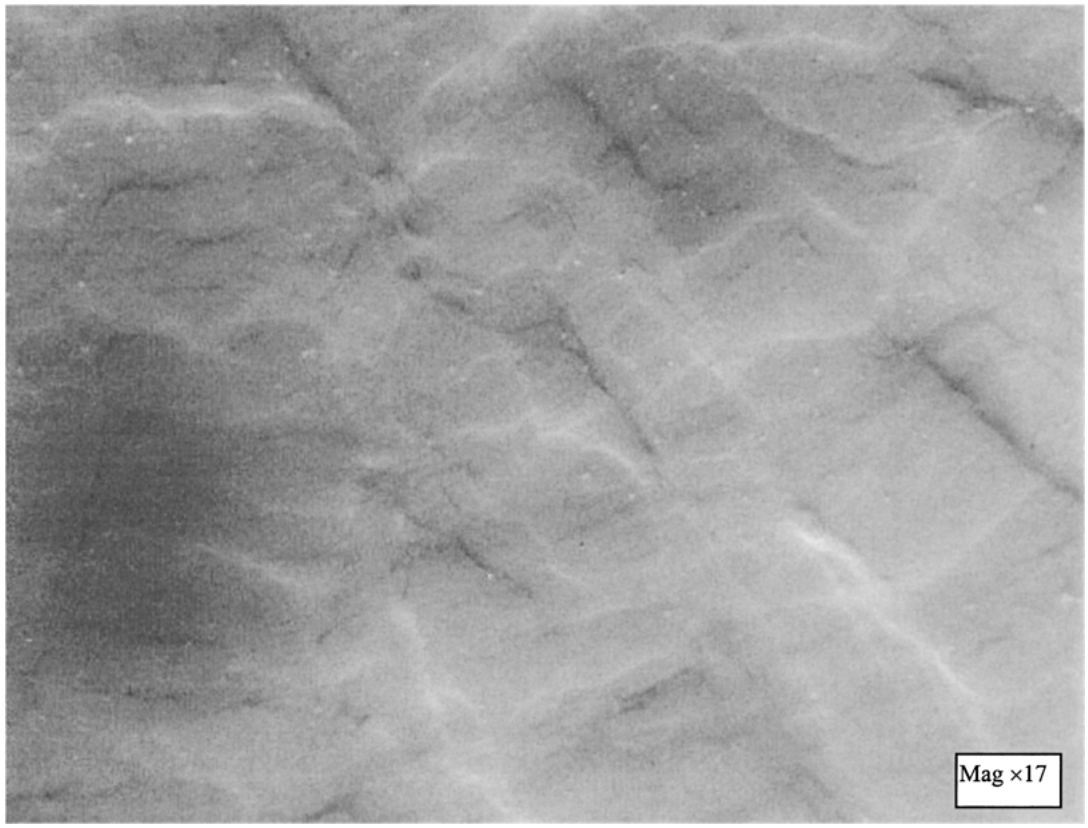

Figure 9 Optical micrograph of sample surface, compaction temperature 733 ± 20°C.

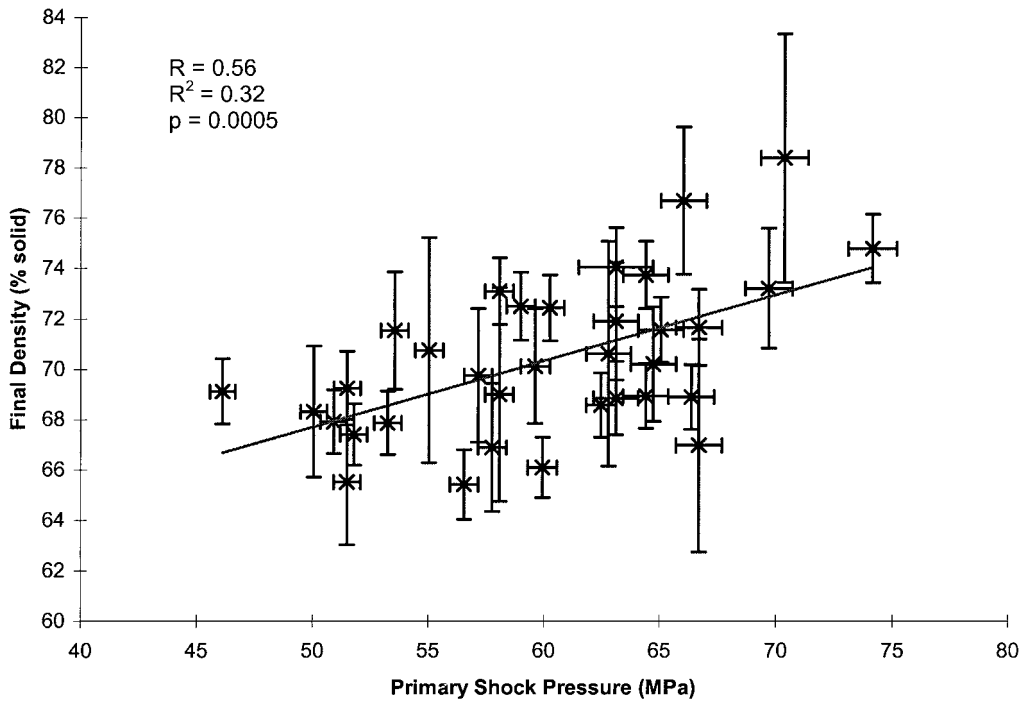

Figure 10 Graph of compact density versus primary shock pressure.

sintered, room temperature, quasi-statically and dynamically compacted samples.

The hardness values for the samples shock compacted at room temperature and then sintered were higher than those for the hot shock compacted samples. This seems reasonable, as the sintering process, which occurred in the hot shock compacted samples, was transient, with the compaction process taking only several hundred microseconds. However, the samples that were shock compacted at room temperature and then sintered were exposed to elevated temperature conditions for approximately 30 min after compaction, while they cooled, allowing more time for diffusional bonding to occur within the sample.

A further point to consider is that the room temperature, shock compacted samples exhibited severe

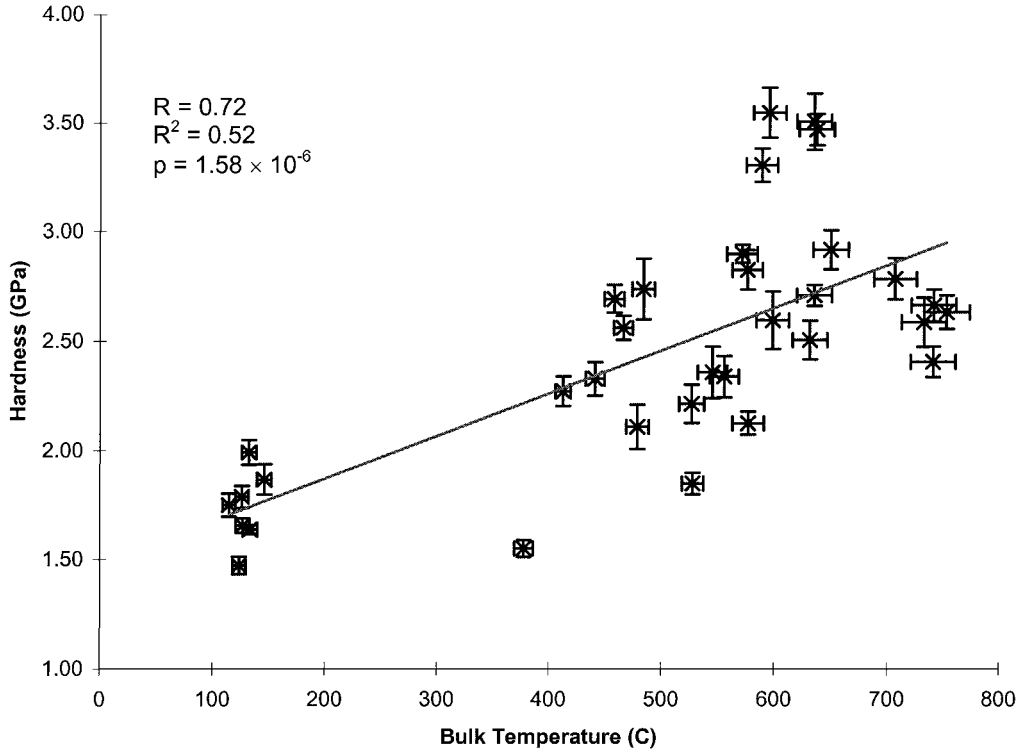

Figure 11 Graph of compact hardness versus compaction temperature for hot shock compacted samples.

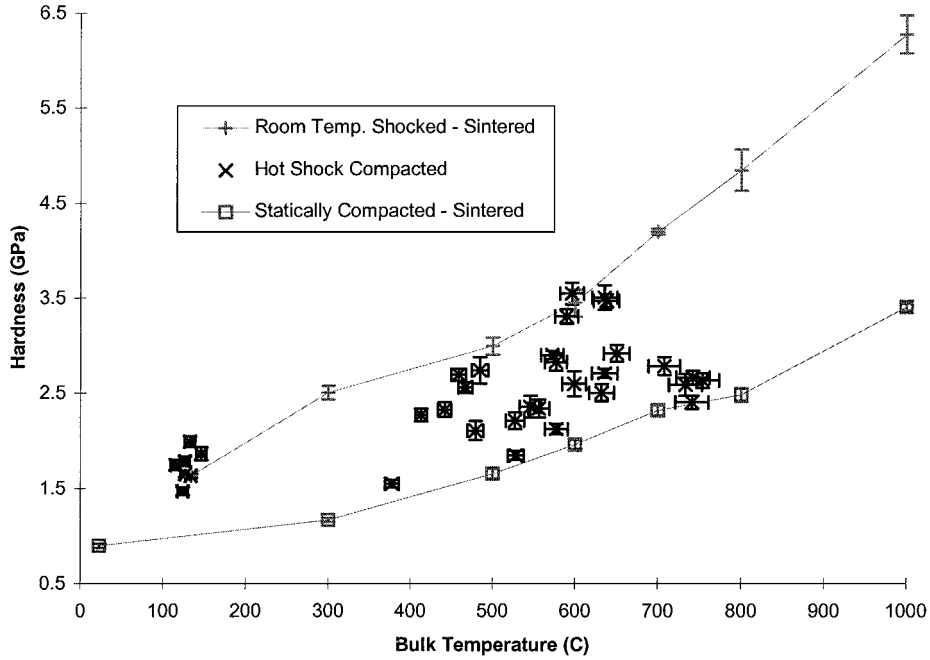

Figure 12 Graph of compact hardness versus temperature for samples produced using each technique.

cracking and were recovered only as fragments. The hot shock compacted samples contained significantly less cracking and were recovered intact, indicating that hot shock compaction is preferable if crack-free materials are to be produced.

Those samples which were statically compacted and then sintered appeared to have lower hardness values than the hot shock compacted samples. However, the density of the quasi-statically compacted samples (∼59% solid density) was lower than that of the hot shock compacted samples (∼66–75% solid density), so care must be taken when comparing the two.

It should be noted that quasi-static compaction at a pressure of ∼980 MPa resulted in densities of ∼59% solid density, whereas room temperature shock compaction at pressures of 62–64 MPa produced densities of 66–75% solid density. Shock compaction is therefore more effective in producing high density compacts than quasi-static compaction.

4. Conclusions

Hot shock compaction of nanocrystalline alumina was carried out using a range of shock pressures and

temperatures. A significant reduction in cracking was observed within samples as compaction temperature increased. It was shown that final compact density increased with primary shock pressure, but was not affected by compaction temperature. Hardness, and therefore bonding, increased with both compaction temperature and primary shock pressure, with compaction temperature being the more significant of the two variables.

A comparison was made between hot shock compacted samples, those produced by room temperature shock compaction followed by sintering, and those produced by room temperature static compaction followed by sintering. The results suggested that the most effective of the three techniques in producing dense, well bonded, crack free nanocrystalline ceramic materials was hot shock compaction. Furthermore, both shock compaction techniques were found to be superior to quasi-static compaction in producing materials with high densities, for a given compaction pressure.

Acknowledgments

The authors wish to thank the technical staff of the Science Faculty workshop at QUT for their assistance in the construction of the experimental apparatus used in this research. They also wish to acknowledge the Australian Government and QUT for their financial support in the form of an Australian Postgraduate Award (APA) scholarship.

References

1. J. KARCH, R. BIRRINGER and H. GLEITER, *Nature* **330** (1987) 556.
2. M. CIFTCIOGLU and M. J. MAYO, "Superplasticity in Metals, Ceramics, and Intermetallics" (Materials Research Society, Pittsburgh, Pennsylvania, 1990) p. 77.
3. M. J. MAYO, R. W. SIEGEL, A. NARAYANASAMY and W. D. NIX, *J. Mater. Res.* **5** (1990) 1073.
4. C. SURYANARAYANA, *Int. Mater. Rev.* **40** (1995) 41.
5. J. FREIM, J. McKITTRICK and W. J. NELLIS, *Metall. and Mater. Trans.* A **26A** (1995) 2503.
6. K. KONDO, S. SOGA, E. RAPOPORT, A. SAWAOKA and M. ARAKI, *J. Mater. Sci.* **21** (1986) 1579.
7. C. A. BRUCH, *Ceramic Age* (1967) 44.
8. S. C. GLADE and N. N. THADHANI, *Metall. and Mater. Trans.* A **26A** (1995) 2565.
9. W. H. GOURDIN, *J. Appl. Phys.* **55** (1984) 172.
10. M. A. MEYERS, "Shock Waves for Industrial Applications" (Noyes Publications, Park Ridge, New Jersey, 1988) p. 265.
11. S. SHANG, K. HOKAMOTO and M. A. MEYERS, *J. Mater. Sci.* **27** (1992) 5470.
12. T. TANIGUCHI and K. KONDO, *Adv. Ceram. Mater.* **3** (1988) 399.
13. S. L. WANG, *et al.*, *J. Mater. Sci.* **23** (1988) 1786.
14. A. FERREIRA, M. A. MEYERS, N. N. THADHANI, S. N. CHANG and J. R. KOUGH, *Metall. Trans.* **22A** (1991) 685.
15. A. FERREIRA, M. A. MEYERS and N. N. THADHANI, *ibid.* **23A** (1992) 3251.
16. W. CHEN and S. G. MALGHAN, *Powder Technology* **81** (1994) 75.
17. N. W. PAGE, in Proceedings of the 15th International Symposium on Shock Waves and Shock Tubes, The University of California, Berkley, July 28–August 2 1985 (Stanford University Press, 1986) p. 878.
18. M. W. PETRIE and N. W. PAGE, *J. Appl. Phys.* **69** (1991) 3517.
19. N. W. PAGE, *Shock Waves* (1994) 73.
20. J. R. FITZSIMMONS, The Investigation of Dynamically Compacted High Temperature Superconducting Ceramics—PhD Thesis, School of Physical Sciences, Queensland University of Technology, Brisbane, 1999.

Received 17 April 2002
and accepted 21 March 2003